

Beamwidth Clustering-based Time Evolving MIMO Channel Modelling for Coordinated Outdoor Wireless Small Cells Communications

¹ILLA KOLANI, ²FRANCOIS ZOUGMORE, ³TCHAMYÉ BOROZE, ⁴BAREREM MAO
, ⁵SAVADOGO MOUMOUNI

¹Wireless and Convergence, ²LAME, ³CIC, ⁴CIC, ⁵Telecel BF

¹Telecommunication Engineering and Research Institute University

²University of Ouagadougou, ³University of Lomé, ⁴University of Lomé, ⁵University of Ouagadougou
Lomé, Ouagadougou, Lomé, Lomé, Ouagadougou

¹TOGO, ²BURKINA FASO, ³TOGO, ⁴TOGO, ⁵BURKINA FASO

ilabbeni@gmail.com, zougfran2013@gmail.com, tboroze@univ-lome.tg

Abstract: - In this paper we study a new methodology in MIMO channel modeling based on scattering ring beamwidth- clustering. We demonstrate how small cell MIMO channel correlation is estimable under a relative virtual displacement of scatters by assigning a cluster of beamwidth to an arbitrary small cell. As the virtual displacement of scatters results straightforward to a dynamic re-organization or distribution of scatters around the scattering environment, dynamic probability function (PDF) of beamwidth are foreseen to derive the channel properties. First, we observe in asymptotical analysis that the reference model and the Uniform PDF scattering channel model are two extremes cases of the same version of dynamic scattering normal PDF. We further lay on this particular feature of assigning an arbitrary geometrical parameter of cluster to a small cell, to extend the channel model to a full and complete time-evolving channel for MIMO transmission modes(TM) adaptive control design. Indeed, we also extract an optimal switching criterion for both spatial multiplexing TMs and transmit diversity TMs by deriving the point of inflection of the multiplexing function under the channel correlation constraint. Finally, using Vienna Institute LTE –A simulator, simulation results in terms of BLER and Throughput for different receivers Zero Forcing (ZF), Minimum Mean Square Error (MMSE) and Soft Sphere Decoding (SDD) are provided, corroborating the study.

Key-Words: - MIMO Adaptive, Small cell, Reference Model, Beamwidth, Transmission Mode, PDF, Dynamic Scattering.

1 Introduction

Modeling MIMO time-variant channels as real world of wave propagation environments dictates becomes crucial in wireless communication. The first ‘open problem’ is to shape a MIMO channel model that evolves with the motion of the UE and at the same time performing the selection of the optimal MIMO signal processing. Indeed, differentiation is required among transmit diversity, spatial multiplexing and beamforming –based TMs, so the capability of the eNodeB to dynamically and optimally select the

MIMO TM that matches the channel conditions will be a key focus for 5G networks.

However, until the release 9, it has been observed [3] that the 3GPP is silent about on whether switching scheme can be performed. For instance, the LTE channel model specified by the 3GPP is an Extended (ESCM) version of the SCM amputated of the time evolution features or the concept of ‘drops’[19][20] . Consequently, the channel is specified and limited for well-known and fixed propagation environments A, B, C, and D [21]. However realistic scenario suggests dealing with the motion of the mobile and then fast fading scenario.

Moreover with the advent of the release 10, TM9 becomes the opened–discussion since this transmission mode should support the spatial multiplexing and beamforming SU-MIMO/MU-MIMO switching on the rank 1 basis.

The second ‘open problem’ is to conceive the format of the channel state information (CSI) that could be efficiency exploited at the transceiver for optimal signal processing. However the tracking of full CSI requires accurate channel impulse response and the knowledge of instantaneous location of the UE. This may be feasible in slow fading scenario but not in fast fading where the feedback mechanisms often generate a delay in receiving information and thus the loss[1][2]in throughput. However instead of having unreliable and inefficiency instantaneous channel state information, a transceiver can efficiency exploit the partial channel state information (PCSI) referred to as the channel covariance or correlation [3].

In general correlations characteristics can be obtained either by field measurements or geometrical stochastic channel modeling [4].Mainly because of their relative simplicity, accuracy and suitability in any propagation environment, geometrical based MIMO channel modeling is used for wireless performance analysis. For instance, standard MIMO channels as 3GPP Spatial Channel Model (SCM) and WINNER Models [5]-[10] and non-standard channels [11]-[18] are driven from this framework. The main lack and limitation of geometrical based models resides in the fact they are most suitable to describe stationary scenario of the channel.

In this paper, both challenges are studied and discussed. Our contribution is in three folders: first we examine a new channel modeling for small cell wireless communications taking into account the stochastic features introduced by the rapidly time variant component .Indeed consider each drop as the channel realization $R(\alpha_n)$ observed as instant t within a given small cell scattering environment S_N . At $t+dt$, following to the motion of the mobile, the channel realization experiences $R(\alpha_{n+1})$, α_n denoting the beamwidth seen at the base station and generated from the scattering system S_N and. Finally $R(\alpha_n)$ is distributed following the distribution $\alpha_n = [\alpha_1, \alpha_2, \alpha_3, \dots, \alpha_{max}]$. The channel R is then estimated by averaging upon the overall channel realizations following a given Probability Density Function (PDF) of beamwidth. Second, by assigning an arbitrary geometrical parameter of a cluster to a small cell coverage, we extend the channel model to a full and complete time-evolving channel for MIMO

transmission modes(TM) adaptive control purpose. Finally we propose a MIMO transmission mode switching criterion based on the formulated channel.

The organization of the paper is as follows: Section 2 formulates the channel model format, in section 3, the time evolving channel modeling is investigated. In section 4 we present the model in details and analyze the correlation properties with existing reference model. Section 5 introduces an advanced MIMO TM selection. Section 6 implements the switching algorithm. In section 7 we present simulation results corroborating our studies. In section 8 we summarize the study.

2 System Model formulation

2.1 Small Cell Concept

The concept small cell as its name indicates, suggests a small area of coverage of access an access point. Hence microcell, microcells, picocells, femtocells, relay nodes and WiFi access points are commonly considered as small cells[41] characterized by the shortness of the radius in comparison with macrocells.

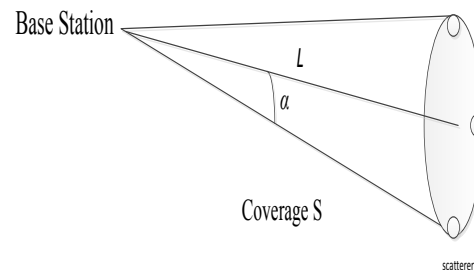


Fig. 1 typical small cell: Coverage-based beamwidth

Herein, the coverage radius is not necessary a sufficient condition.

Let assume a typical form of a coverage determined by a beamwidth generated by scattering ring of radius r , α can be given as:

$$\alpha = \text{tang}(r/L) \quad (1)$$

From (5), it is clear the smallness of α hold as long as L is high and the coverage determined by the beamwidth is depending on both radius r and L .

We define a small cell as a cell with a short coverage shaped by a given geometry of scatterers. From this definition it will be possible to envisage small cell with short radius L as well as small cell with L relatively high.

2.2 Stationary channel Modelling

Let us consider a MIMO channel H with n_t transmit and n_r received antennas, we can define the correlation between channel H random entries by the correlation matrix R as:

$$R = \varepsilon \{ \text{vec}(H) \text{vec}(H)^H \} \quad (2)$$

ε denotes the expectation and $(.)^H$ the conjugate transpose. When R is known, H can be computed as:

$$H = G.R^{1/2} \quad (3)$$

R can explicitly be written in terms of matrix where an arbitrary element $r_{kl,qs}$ stands for a correlation between two arbitrary multipath channels $h_{kl}(t, f)$ and $h_{qs}(t + \Delta t, f + \Delta f)$ defined by antennas k, q at the receiver side array and antennas l, s at the transmitter array. It should be noted that $k, q \in [1, n_r]$ and $l, s \in [1, n_t]$

Let's assume a transceiver within a subsystem n . Under the assumption of Wide Sense Stationary Uncorrelated Scattering (WSSUS) process, we can write:

$$r_{kl,qs} = F(\Delta t, \Delta f) \quad (4)$$

where F denotes a specific function which depends on the geometry (sub-system) formed by scatterers around the transceiver and the resulting distribution of Angle of Arrival (AOA) and Angle of Departure (AOD). Δt and Δf respectively stand for time and frequency lags between two arbitrary MIMO sub channels.

Since $r_{kl,qs}$ is geometrical-based scattering model, without lose any generality, let's introduce a parameter α of the geometry. We may rewrite:

$$r_{kl,qs} = r(\Delta t, \Delta f, \alpha) \quad (5)$$

Notice that (3) describes a stationary state and then is only suitable to illustrate correlation for fixed transceiver (or relative fixed scattering environments). We assume here α delimits a small coverage area that fits small cell concepts.

2.3 Fading Scenario

Let's now consider a scattering environment system S_m . The relative mobility of scatterers implies a relative and virtual displacement of scatters and then a dynamic re-organization around the ring, introducing straightforward a stochastic feature.

Within a given subsystem n , let's associate the corresponding channel correlation:

$$r_{kl,qs}^n = F(\Delta t_n, \Delta f_n, \alpha_n, \nu_n) \quad (6)$$

Following the motion of the mobile, the correlation $r_{kl,qs}^n$ may be born and died during each drop evoking the concept of birth and death described in [22]. Therefore, $r_{kl,qs}$ experiences many intractable realizations and as consequence of contribution by all possible N channel realizations, (6) can be extended as follows:

$$\overline{r_{kl,qs}} = \frac{1}{N} \sum_{n=1}^N nF(\Delta t_n, \Delta f_n, \alpha_n, \nu_n) \quad (7)$$

Where $r_{kl,qs}$ denotes the average correlation upon the overall channel realization $r_{kl,qs}^n$. As consequence it should also be noted that from (7) $\overline{r_{kl,qs}}$ will be a function of a typical form beamwidth referred to as effective beamwidth α_{eff} .

Equation (7) tempts to estimate the channel in fast fading but do not bear any time-evolving characteristic.

3 Time-Evolving Channel Model

Let's now consider a base station where each cell is equipped with multielement antenna transmission systems. Let's consider the coverage area dividable in to m small cells $S_m \{m = 1, 2, 3, \dots, m\}$, each one governed by multi ring scattering objects given by (7). Let us rewrite the channel properties for an arbitrary small cell S_m as $r_{kl,qs}|_{S_m}$, therefore

accordingly to the motion of the mobile over small cells $S_m \{m = 1, 2, 3, \dots, m\}$, the time- evolving channel $r_{kl,qs}(t)$ of the cell is deduced as:

$$\overline{r_{kl,qs}}(t) = \overline{r_{kl,qs}|_{S_m=S_1, S_2, \dots, S_m}} \quad (8)$$

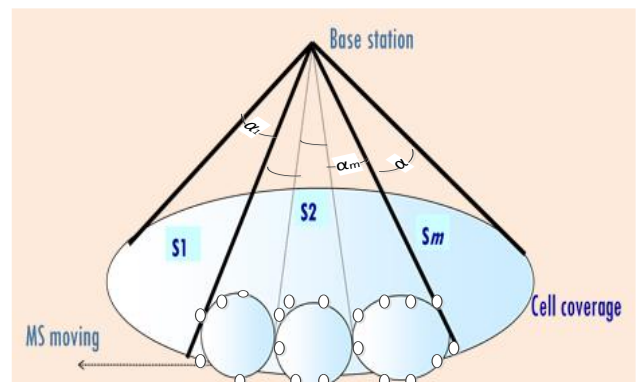


Fig 2 small cell channel model

Since parameters Δt and Δf depend on the choice of coding perspective than scattering environments and the velocity ν on the user prerogative,

$\overline{r_{kl,qs}}_{|S_m=S_1, S_2, \dots, S_m}$ estimation will turn therefore to estimate the physical beamwidth as :

$$\alpha_{eff}(t) = \alpha_{eff}(m) \tag{9}$$

Eq (8) postulates $\overline{r_{kl,qs}}(t)$ as the sum of stationary channels $\overline{r_{kl,qs}}_{|S_m}$. For a given MIMO configuration, the cell channel $\overline{r_{kl,qs}}(t)$ can be estimated through the codebook $\overline{r_{kl,qs}}_{|S_m=S_1, S_2, \dots, S_m}$.

MIMO TM Switching Mechanism Model

We examine in this section to a new formulation of MIMO transmission modes adaption by study the influence of channel state on the performance of MIMO systems.

$\overline{r_{kl,qs}}_{|S_m=S_1, S_2, \dots, S_m}$ is a typical form of partial channel state information (CSI) which can be exploited at the base. Within each small cell, for an $n_t \times n_r$ MIMO configuration, the base station will need to estimate within the channel correlation R , $n_t \times n_r (n_t \times n_r - 1)$ elements of $\overline{r_{kl,qs}}$, handling $n_t \times n_r (n_t \times n_r - 1)$ elements can become huge for $n_t \times n_r$ high. Hence, to dispense

$$R = \begin{pmatrix} 1 & \overline{\eta_{1,21}} & \overline{\eta_{1,12}} & \overline{\eta_{1,qs}} & \dots & \overline{\eta_{1,n_t n_r}} \\ \overline{\eta_{1,21}}^* & 1 & \overline{\eta_{2,12}} & \overline{\eta_{2,qs}} & \dots & \overline{\eta_{2,n_t n_r}} \\ \overline{\eta_{1,12}}^* & \overline{\eta_{2,21}} & 1 & \overline{\eta_{2,qs}} & \dots & \overline{\eta_{2,n_t n_r}} \\ \overline{\eta_{1,qs}}^* & \overline{\eta_{kl,21}} & \overline{\eta_{kl,12}} & 1 & \dots & \overline{\eta_{kl,n_t n_r}} \\ \vdots & \ddots & \ddots & \ddots & \ddots & \vdots \\ \overline{\eta_{1,n_t n_r}}^* & \overline{\eta_{2,n_t n_r}} & \overline{\eta_{2,n_t n_r}}^* & \overline{\eta_{kl,n_t n_r}}^* & \dots & 1 \end{pmatrix}$$

with the study of the effect each element, we will utilize the correlation measure metric of the total of correlation $\psi_{n_t n_r}$ [34][35] which performs an average on the overall element. Notice that high (resp. low) amount of correlation implies high (resp. low) correlated and its value extends from 0 to 1.

Let's now investigate the error rate and capacity performances of MIMO in terms of its diversity g_d and multiplexing gain g_s . The impact of the channel quality on both performances will be described by:

$$g_s = f(g_d, \psi_{n_t n_r}) \tag{10}$$

Note that equ (10) rely the three fundamental parameters of MIMO systems.

Proposition

Consider a base with both *transmit diversity* (tx_d) and *spatial multiplexing* (tx_sm) capability. For an $n_t \times n_r$ MIMO configuration within a given channel condition $\psi_{n_t n_r}$, if $g_s(tx_d) > g_s(tx_sm)$, ENABLE *transmit diversity* transmission modes.

Proof

Spatial multiplexing transmission modes are capacity-motivated MIMO while *transmit diversity* transmission modes are error-motivated MIMO design, hence $g_d(tx_d) > g_d(tx_sm)$ hold always.

If moreover $g_s(tx_d) > g_s(tx_sm)$, *transmit diversity* transmission modes is optimally performing in both diversity and multiplexing gain.

4 Practical Channel Model

4.1 Reference Model

Thanks to its accordance with experimental result [23][24], the one ring scattering model is considered suitable to simulate narrow band communication systems as well as communication system using MIMO- OFDM scheme. In this model, it is assumed that a fixed mobile station is surrounded a ring of scatterers while the base station is elevated and not obstructed (Fig.1).

Considering a parallel Uniform Linear Array (ULA) antenna between the transmitter and the receiver, employing a uniform Probability Density Function (PDF) of Angle of Arrival (AOA) and following the method of computation used in [25][Appendix I], we derive the general formulation of the correlation function in an arbitrary one ring scattering with a given radius r as :

$$\overline{r_{kl,qs}}(\Delta t, \alpha, f_d) = e^{j2\pi \frac{d}{\lambda}(s-l)} J_0 \left(2\pi \left(\frac{D}{\lambda}(q-k) + \frac{d}{\lambda} \alpha(s-l) + f_d \Delta t \right) \right) \tag{11}$$

Where D , d and λ denote respectively the antenna spacing at the base station, at the mobile station and the wavelength. $f_d = v/c$ is the maximum Doppler spectrum, α stands for a parameter that is related to the geometry (ring) formed by scatterers. It is also referred to as the beamwidth seen at the base station and is given as (1). As reflected in (11), the reference

model is suitable to describe the behavior of non-frequency selective channels.

4.2 Proposed Dynamic Scattering Channel

In this section we will focus on the elaboration of a channel model taking into account dynamic scattering aspect.

As a template, the one ring scattering model will be considered. An arbitrary scattering ring n wherein the correlation properties is given by $r_{kl,qs}(\Delta t_n, \alpha_n, f_d_n)$. Assuming a constant velocity v and time lags (which can be seen as symbol period T_s), it follows that the variation of $r_{kl,qs}(\Delta t_n, \alpha_n, f_d_n)$ with time or the motion of the mobile, induces its variation with α_n . Indeed, from (1), $\alpha_n = \tan\left(\frac{r_n}{L_n}\right)$ (r_n and L_n stand respectively for the radius of the scattering ring and the distance between the base and the mobile) depends on the distance between the base –mobile and the radius of the scattering ring, both parameters are subject of variation following the motion of the mobile. Consequently the channel will experience the distribution $r_{kl,qs}(\Delta t, \alpha_n, f_d)$ with $\alpha_n = [\alpha_1, \alpha_2, \alpha_3, \dots, \alpha_N]$.

The expectation $\overline{r_{kl,qs}}$ of $r_{kl,qs}(\Delta t, \alpha_n, f_d)$ can be written following (4) as:

$$\overline{r_{kl,qs}} = \frac{1}{N} \sum_{n=1}^N n \cdot r_{kl,qs}(\Delta t, \alpha_n, f_d) \quad (12)$$

- In (12), n/N can be interpreted as the probability p_n of the of the correlation matrix channel $r_{kl,qs}(\Delta t, \alpha_n, f_d)$ to be occurred.
- According to the experiments result leaded at different locations and frequencies in[26]-[32] the beamwidth α_n seen at the base in an arbitrary one scattering ring scenario is generally small, most often than 15° , and some case, very small, less than 5° .
- Hence, within the coverage zone of a small cell, the range of the values that can be taken by the beamwidth is $\alpha_n = [\text{tang}(0^\circ) \text{ tang}(15^\circ)]$.

4.2.1 Uniform Distribution of Beamwidth

In this section, we will assume that an arbitrary scatterers S_N has the same probability to be born and died. Therefore a uniform distribution of beamwidth can be approximated by assuming the mobile moving through a limited number of group of scatterers. In this scenario, the formula (12) can be rewritten as:

$$\overline{r_{kl,qs}} = \frac{1}{\alpha_1 - \alpha_{\max}} \int_{\alpha_1}^{\alpha_{\max}} r_{kl,qs}(\alpha_n) d\alpha_n \quad (13)$$

From (10) we found $\overline{r_{kl,qs}}$ as following:

$$\overline{r_{kl,qs}} = e^{j2\pi(s-l)\frac{d}{\lambda}} \frac{\lambda}{2\pi d(s-l)\alpha_{\max}} \left[J_0\left(2\pi\left(\frac{D(q-k)}{\lambda} + f_d \Delta t\right)\right) \sum_{k=0}^{\infty} J_{2k+l}\left(\frac{2\pi}{\lambda} d(s-l)\alpha_{\max}\right) \right] \quad (14)$$

$k, q \in [1, n_t]$ and $s, l \in [1, n_r]$
 $k - q \geq 0$ and $s - l \geq 0$

More about the formulation of (12) can be seen from the appendix

4.2.2 Normal Distribution of Beamwidth

Gaussian distribution has many interests because of its accuracy and suitability in many systems dealing with infinite numbers. This approach can be also used in multiple scattering ring channels.

For N large [17], the central limit theorem allows to approximate (12) by the integral form:

$$\overline{r_{kl,qs}} = \int p_n \cdot r_{kl,qs}(\alpha_n) d\alpha_n \quad (15)$$

With

$$d\alpha_n = \frac{2c}{\sqrt{\pi}} e^{-c^2(\alpha_n - \alpha_0)^2} \quad (15)$$

where α_0 represents the location of the peak of $d\alpha_n$. Note that c can be chosen in order to ensure that d_n decreases rapidly beyond the interval of α_n . We found the cross-correlation from (15):

$$\overline{r_{kl,qs}} = \frac{1}{\sqrt{\pi}} e^{j2\pi(s-l)d/\lambda} \cdot J_0\left(2\pi\left(\frac{D(q-k)}{\lambda} \pm f_d \Delta t\right)\right) \mathbf{X} \cdot J_0\left(\frac{2\pi}{\lambda} d(s-l)\alpha_0\right) \mathbf{X} \sum_{m=0}^{\infty} \frac{(-1)^m \Gamma(m + \frac{1}{2})}{(2c)^{2m} (m!)^2} \quad (17)$$

The transmit correlation is obtained:

$$\overline{r_{kl,ks}} = e^{j2\pi(s-l)d/\lambda} \cdot J_0(2\pi f_d \Delta t) \cdot \frac{1}{\sqrt{\pi}} J_0\left(\frac{2\pi}{\lambda} d(s-l)\alpha_0\right) \mathbf{X} \sum_{m=0}^{\infty} \frac{(-1)^m \Gamma(m + \frac{1}{2})}{(2c)^{2m} (m!)^2} \quad (18)$$

Where $\Gamma(x)$ denotes the gamma function. The receive correlation remains unchanged:

$$\overline{r_{kl,ql}} = r_{kl,ql} = J_0 \left(2\pi \left(\frac{D}{\lambda} (q-k) \pm f_d \Delta t \right) \right) \quad (19)$$

4.2.3 Kronecker's Representation validity

Kronecker's model representation of MIMO channel is often considered in correlation-based and analytical based MIMO channel modeling because of the simplicity offered in channel representation; the channel is given as:

$$H = R_r^{1/2} G R_t^{1/2} \quad (20)$$

From this perspective, handling the correlation R turns to handle transmit and receive correlation separately.

Let's investigate the validity of this assumption, the requirement for a MIMO channel to be seen as Kronecker's model is given in [33] as:

$$\overline{r_{kl,qs}} = \overline{r_{kl,ks}} \cdot \overline{r_{kl,ql}} \quad (21)$$

Discussion

- Clearly it can be observed that equations (14), (17) do not respect the requirement of (21).
- Let's now consider the case of static channel or quasi-static channel, the multi element antenna system is fixed or moving slowly ($f_d \Delta t \approx 0$) within multiple scattering rings. We may state $J_0(2\pi f_d \Delta t) \approx 1$, then the relationship in (21) holds.
- Antennas largely spaced may induce a Kronecker's representation of MIMO channel. Indeed, let's consider a systems with 2 antennas spaced by $(q-k)D$ at the receiver and two antenna spaced $(s-l)d$ at the transmitter in antenna arrays as ULA. In equation (14), (17), it is obvious that when $(q-k)$ and $(s-l)$ is large as well as possible, the relation (13) holds fulfilling the Kronecker's requirement.
- Let's assume α_0 large, the close form of Kronecker's model is respected; however, this is utopic due to the fact that α_0 is specified not exceeding 15° .
- Antennas largely spaced induce a Kronecker's representation of MIMO channel.

4.2 Correlation Properties of channels

4.2.1 Key Parameters of the Channel Model

One of the main useful parameter that should be estimated in dynamic one ring scattering channel (DORSC) as well as in a one ring scattering channel is the beamwidth. However the characteristic of this parameter is not necessary similar in different channels models. In the reference model, α defines uniquely the beamwidth seen at the base while α_0 and α_{max} are effective beamwidth. α_0 and α_{max} respectively specify the value of the angle spread α for which the peak of number of scattering rings is reached and the maximum value of the beamwidth seen at the base respectively in Gaussian distribution and in uniform distribution. The method of estimation α is described in [26]-[32] for the reference model.

For the Gaussian PDF based DORSC, α_0 as well as the nature of the parameter of dispersion c can be estimated following the same process, however the experimental measurements should be done repeatedly and by changing the position of the mobile station within the specified environment S_N .

In case of using the uniform PDF based channel model it can be recommended to adopt $\alpha_{max} = 15^\circ$ without any need of experimental measurements since previous experimental results show $\alpha = [0^\circ \ 15^\circ]$.

4.2.2 Channels Performances

In this section, we analyze channels performance in terms of their correlation proprieties. 2x2MIMO and 4x2 MIMO antenna configurations channels performances are simulated in a dynamic

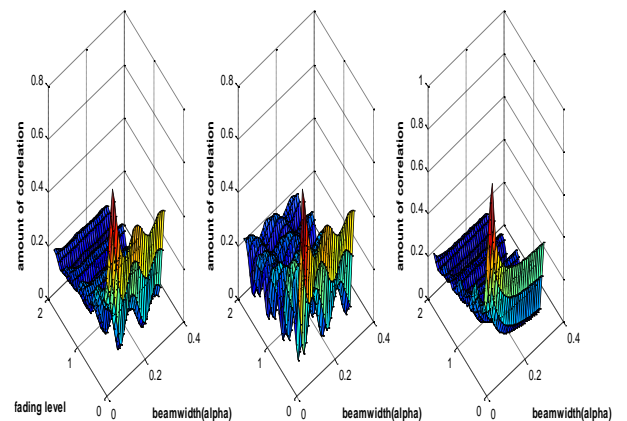


Fig.3: 2x2 MIMO correlation properties, (a) in Gaussian PDF (b) in the reference model, (c) in Uniform PDF

scattering environment system assuming both Gaussian PDF and Uniform PDF (fig.3). Both performances are in compared with the one- ring scattering channel. The following the parameters of the beamwidth $\alpha_{eff} = \alpha_0 = \alpha_{max}$.

The antenna spacing are $D = 2\lambda$ at the eNodeB and $d = 0.2\lambda$ at the mobile where $\lambda = 1/2\text{GHz}$ denotes the wavelength (working frequency) as specified in LTE transmission system.

In can be observed that, correlation levels in different scattering channel scenario decrease with the increase of the beamwidth and the fading speed. However some similarities can be depicted. Indeed, the amount of correlation in Dynamic scattering Gaussian PDF model behaves approximately as a translation (by a given factor) of the amount of correlation of the reference model in fading level $f_d\Delta t \leq 1$ (slow fading), however in fast fading $f_d\Delta t > 1$, it behaves similarly as in uniform PDF dynamic scattering rings. Therefore, we deduce that the reference model and the Uniform PDF scattering channel model are two extremes case of the same version of dynamic scattering Gaussian PDF.

5. Dynamic Adaptive MIMO TM

5.1 Problematic of LTE/LTE-A TM Switching

For next generation of mobile networks as 5G networks, the physical layers will be mapped into multiple transmission modes(TM) and each TM should be dynamically selected depending on the time-varying MIMO channel. Besides the single antenna SISO transmission (TM1), multielement antenna (MIMO) technology such as Open Loop

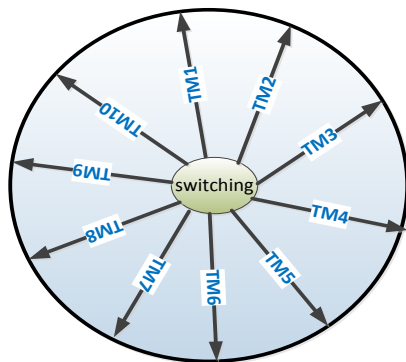


Fig.4 Transmission Modes in release 10

Spatial Multiplexing (OLSM) and Close Loop Spatial Multiplexing (CLSM) transmissions are also specified in release 9 by the 3GPP standard for LTE/LTE-A transmission (fig.4). TM1 indicates the single antenna port transmission SISO (Single Input Single Output); TM2 and TM6 denote respectively transmit diversity also referred to as open loop spatial multiplexing (OLSM) and close loop spatial multiplexing (CLSM) where in both case one data stream is transmitted (Rank 1); TM3 and TM4 are respectively OLSM and CLSM, both consisting in transmitting two (rank2) data streams. TM7, TM8 implement one layer beamforming and dual layer beamforming. In practice, most of mobile communications deal with multi users sharing the same resources. Hence, a high diversity gain can be achieved by scheduling to users in high channel quality conditions. This technic is commonly known as multi-user diversity or TM5. TM9 and TM10 enable multiple layers transmission up to 8 layers in 3GPP Release 10.

5.2 MIMO TM Switching Processing

A complete switching scheme design involve taking to account MIMO channel keys parameters indicator. In this section we first analyse characteristics of environment favourable or unfavourable to a given transmission mode, further we re-visit the Rank Indicator (RI) formulation accordingly to equation (8) and switching criterion.

5.2.1 Transmission Modes strength and weakness

In this section we first browse the strength and weakness of OLSM and complete the analysis with CLSM processing in regards with the whims of MIMO time-varying Channel.

5.2.1.1 TM based on SISO and MISO

Although transmissions are expected to be fully based on MIMO, the transmission through a SISO channel is also possible. In principle, SISO can be enabled in case of bad MIMO channel condition or one-rank scenario. In this case of *degenerate MIMO channel*, the utilization of MIMO features become wasting resources. Indeed, this channel condition corresponds to high MIMO channel correlation level or the amount of correlation threshold (see Fig.5) from which the diversity gain of MIMO, either coincides (MIMO Orthogonal Space Time Block Codes) SISO channel or decreases (MIMO spatial multiplexing) below that of SISO channel. Expectedly this channel condition is also favourable

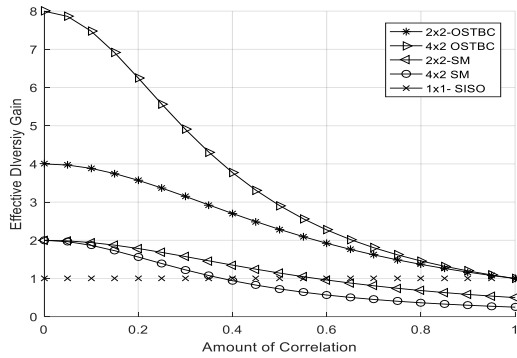


Fig.5 Amount of correlation versus diversity gain, multiplexing gain=0

to beamforming rank 1 TM6 which can be enabled, however with the requirement of the knowledge PMI.

5.2.1.2 Environments Favorable to OLSM

In this group, we may distinguish TM2 or OLSM rank 1 which implements the well-known Alamouti transmit diversity transmission mode implementable with 2 transmit antennas (2x_{n_t},MIMO). However Alamouti scheme is a simple version of orthogonal space-time block coding (OSTBC). This transmission technic does not necessary require the knowledge of CSI or PMI feedback. As shown in fig 5 the robustness of both beamforming and transmit diversity remains high even in high correlation A Special case of spatial multiplexing is implementable and without strictly need of the full knowledge of CSI. With the support of diversity through LD-CDD precoders this type of transmission mode is denoted as TM3 or OLSM rank 2. From figure 7, OLSM rank 2 multiplexing gain is guaranteed in low correlation

$$\Psi_{n,n_r}$$

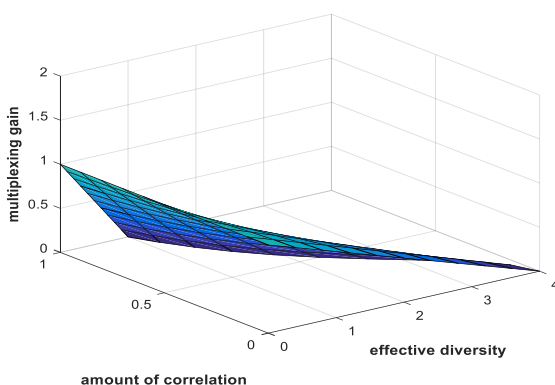


Fig.6 2x2 MIMO rank 1 multiplexing gain versus effective diversity gain in the presence of correlation

5.2.1.3 Environments Favorable to CLSM

This group of transmission requires the full knowledge of the CSI or PMI feedback. In this group differentiation is made between CLSM rank 1(TM6), beamforming rank 2(TM7) and CLSM rank 2 (TM4). CLSM rank1 and TM7 implement beamforming, its

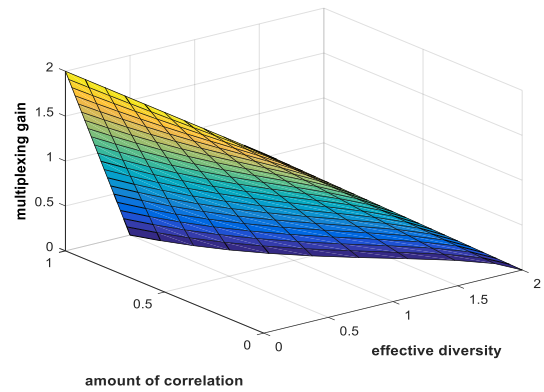


Fig.7 2x2 MIMO rank 2 multiplexing gain versus effective diversity gain in the presence of correlation

diversity can be strengthened in the presence of high correlation. In contrast, CLSM rank 2 multiplexing gain is guaranteed only in low correlation environment (fig 7).

5.2.2 Adaptive TM Switching Strategy

The TM switching point can be first investigated in terms of *group of transmission modes (GT) selection* from which an *inner selection* can be performed.

5.2.2.1 Group of Transmission Modes Selection

As previously mentioned, from the signal processing perspective, differentiation has to be made between GT CLSM and GT OLSM and. The former requires additional precoders whereas the latter can be blindly used for data transfer. Those requirements take form as the *availability of channel state information (CSI)*. Therefore, the knowledge of the CSI level becomes a criterion for enabling a group of transmission (GT) modes. Further the base station can start the *inner selection* criterion within the selected GT of transmission modes.

5.2.2.2 Inner Selection: New RI formulation

The inner selection will consist of providing some KPI for the optimal link adaption strategy, rank indicator and enabling optimal precoders. For

maintaining the link quality of MIMO sub channel acceptable, SNR-based link adaption can be performed. Indeed, each sub channel instantaneously quality is tracked through the Channel Quality Indicator (CQI) mapped into multiple CQI_index and relied to the variation of SNR by a compression function. In practice, the eNodeB requests a Measurement Report (MR) from the UE through the reference signal. By decrypting this MR, the base station has to judge and decides from the CQI_index table (1 to 15) which CQI_index is appropriate for the next transmission. The requested CQI is done fulfilling the requirement of a Block Error Rate ≤ 0.1 . Besides the link adaption, the user can be roughly located for GT CLSM (spatial multiplexing and beamforming) purpose by means of Phase Matrix Indicator (PMI) precoders codebook. However, complete MIMO systems performance hold only when a RI feedback mechanism is also available.

The RI concept is used to estimate the number of useful layers for data transmission. It will be useless to transmit data by two layers whereas the actual channel quality allows only one layer. Herein the philosophy behind the proposed RI mechanism is to continuously adapt the multiplexing gain while keeping an acceptable diversity gain in scattering environments. According to the above proposition the switching criterion in scattering environment with a given correlation ψ_{n,n_r} is as follows:

$$\begin{aligned} \text{If } g_s(tx_d) > g_s(tx_sm), \text{ RI}=1 \quad (18) \\ \text{Else} \quad \text{RI}=2 \end{aligned}$$

Equation (18) can be understood in the sense that it will be resources wasting for the network to continue transmitting spatial multiplexing transmission modes when its multiplexing gain is decreasing below that of the transmit diversity. Figure 8 depicts the

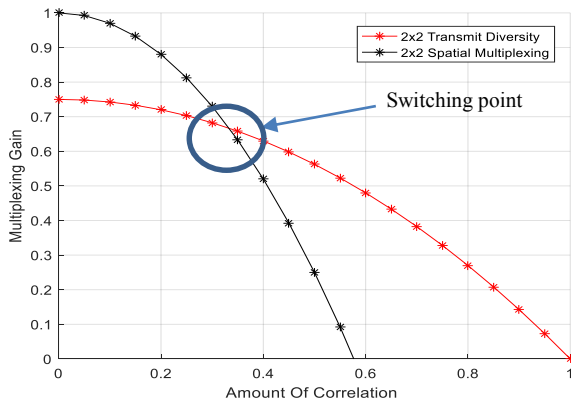


Fig.8 Multiplexing gain versus Amount of correlation for 2x2 MIMO in constant diversity gain =1 (SISO channel)

multiplexing gain for various correlation environments with a constraint of diversity gain ($g^d = 1$); the switching point from which the base can decide for the RI is shown.

6. An Adaptive MIMO TM Algorithm

This section focuses on the implementing of the switching algorithm skeleton. The summarization can be done into two folders:

- The knowledge of the CSI

$$\begin{aligned} \text{If CSI available } TG= \text{ CLSM} \\ \text{Else} \quad TG= \text{ OLSM} \end{aligned}$$

- The RI switching point between MIMO spatial multiplexing and MIMO transmit diversity at threshold1 and switching point at the threshold 2 between MIMO transmit diversity and SISO.

$$\text{If CSI available } TG= \text{ CLSM [TM4, TM6]}$$

For Channel state case= 1:3

$$\text{Case 1, } \psi_{n,n_r} \leq \text{ Threshold 1}$$

$$\text{RI}=2$$

$$\text{PMI} = \text{PMI_index [1 2]}$$

$$\text{CQI} = \text{CQI_index [1 2 3....15]}$$

$$\text{TM} = \text{TM4}$$

$$\text{TM} = \text{TM4} + \text{PMI_index} + \text{CQI_index}$$

$$\text{Case 2, Threshold 1} \leq \psi_{n,n_r} \leq \text{ Threshold 2}$$

$$\text{RI}=1$$

$$\text{TM} = \text{TM6}$$

$$\text{PMI} = \text{PMI_index [1 2]}$$

$$\text{CQI} = \text{CQI_index [1 2 3....15]}$$

$$\text{TM} = \text{TM6} + \text{PMI_index} + \text{CQI_index}$$

$$\text{Case 3; } \psi_{n,n_r} \geq \text{ Threshold 2}$$

Rank one case (bad channel)

$$\text{TM} = \text{TM1}$$

$$\text{CQI} = \text{CQI_index [1 2 3....15]}$$

$TM=TM1+ CQI_index$

Else $TG=OLSM [TM2 TM3]$

For Channel state case= 1:3

Case 1, $\psi_{n,n_r} \leq$ Threshold 1

$RI=2$

$TM= TM3$

$CQI=CQI_index [1 2 3....15]$

$TM=TM3+ CQI_index$

Case 2, Threshold 1 $\leq \psi_{n,n_r} \leq$ Threshold 2

$RI=1$

$TM=TM2$

$CQI=CQI_index [1 2 3....15]$

$TM=TM2+ CQI_index$

Case 3; $\psi_{n,n_r} \geq$ Threshold 2

Rank one case (bad channel)

$TM= TM1$

$CQI=CQI_index [1 2 3....15]$

$TM=TM1+ CQI_index$

End

7. Simulation Results

We consider a normal distribution of beamwidth for simulation purpose. As the switching criterion in terms of the amount of correlation of MIMO channel (see figure 7 and equ 18) can be derived, we first simulate the channel properties (see fig.9) for 2x2 MIMO systems with different antenna spacing $D = t\lambda$, $d = r\lambda$ in different scattering environment α_0 . By utilizing Vienna Institute Simulator[42], we will analyse the transmission error rate and the data rate for two small cells which characteristic α_0 conducts to the channel total of correlation respectively slightly below and above of the switching criterion.

7.1 2x2 MIMO channel properties

Globally the total correlation decreases as both α_0

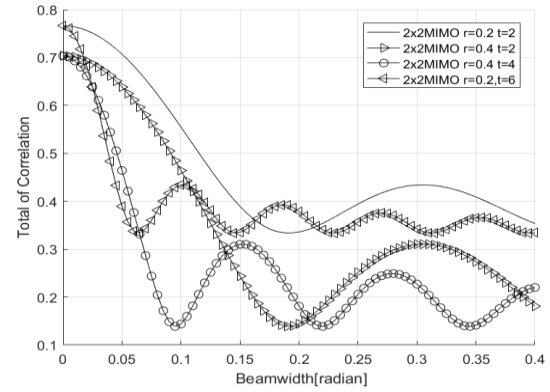


Fig.9 Small cells effective beamwidth versus Channel Correlation $f_d\Delta t \approx 0.2$

and antenna spacing increase. However MIMO systems with high antenna spacing does not conduct directly to low correlation since the total correlation function behaves as a cosine function (better a Bessel function) of variable (see equ 17,18,19). Hence, equ 18, 19 make possible a gauge between α_0 , d and D . In other words, for some values of α_0 , MIMO systems with low amount of correlation can be designed without requirement of high antenna spacing.

7.1 Global Parameters for simulation

The channels are assumed slow fading or quasi static i.e. $f_d\Delta t \approx 0.2$ fulfilling then Kronecker's representation as demonstrated above. The antenna spacing are $D = 2\lambda$ at the eNodeB and $d = 0.4\lambda$ at the mobile where $\lambda = 1/2\text{GHz}$ denotes the wavelength (working frequency) as specified in LTE transmission system. The bandwidth of 20 MHz is considered. We assume that the UE requests the Channel Quality Indicator (CQI) index 10 for both Close Loop Spatial Multiplexing (CLSM)-based LTE/LTE-A transmission mode and Open Loop Spatial Multiplexing (OLSM)-based LTE transmission mode

7.2 Local Parameters for simulation

For a 2x2 MIMO systems with $D = 2\lambda$ at the eNodeB and $d = 0.4\lambda$ at the mobile, we consider a UE with different receiver capability and moving over different cells. The corresponding channel correlation matrix can be generated following (18) and (19). The above table presents the channel characteristic of the same UE in two small cells controlled by the same base station. Within the amount of correlation is below the threshold 1 in the first one, and slightly

above in small cell 2. According to the decision rule availability of the CSI or not. This scenario is

	Small Cell 1	Small Cell 2
Effective beamwidth α_0	0.18	0.1
Channel ψ_{n,n_r}	0.0974	0.405
Threshold 1	0.35	0.35
Switching decision	$\psi_{n,n_r} < \text{Threshold}$ 1	$\psi_{n,n_r} > \text{Threshold}$ 1
Receive Correlation	[1 0.114 0.114 1]	[1.0000 0.114 0.114 1]
Transmit Correlation	[1 0.075 0.075 1]	[1 0.64 0.64 1]

Table: Local parameters

favorable to high data transmission with a reasonable SNR. In contrast, CLSM rank 1 and OLSM rank will be the optimal choice in small cell 2.

7.2 Throughput and BLER analysis.

In this section, transmission modes throughput and Block Error Rate (BLER) are analyzed concomitantly over small cells channels parameters (see above table). We consider in this scenario MMSE (Minimum Mean Square Error), ZF (Zero Forcing) and SDD (Soft Square Decoding) UE receiver capability.

By comparing the group of figures 1, 2 and 3, it is clear that SDD receiver is the most performing receiver, followed by the ZF receiver since it requires less signal to noise ratio in comparison with MMSE. Therefore by focusing on the transmission modes performances through SDD receiver (group of figures 1) we note that in cell 1 OLSM rank 1 as well as for CLSM, rank1 transmission modes remain robust in terms of BLER (BLER < 0.1 in fig.10) while being able to offer their maximum throughput in reasonable Signal to Noise Ratio (throughput in fig.12) around 15 db. Indeed rank 1 TMs are diversity based MIMO signal processing and there will be always performing from low to high correlation, however they do not bear high data rate in comparison with rank 2 transmission modes. Slightly more, around 17 dB will be required for rank 2 transmission modes to exceed the performances of rank 1 modes. In this

posture, the base can simply chose in this favorable channel condition high data transmission i.e. CLSM rank 2 when the CSI is available or OLSM rank 2 when the CSI is not known.

In cell 2 where the amount of correlation is slightly exceeding the decision criterion, rank 2 transmission modes BLER (fig.11) are catastrophic and requires high SNR to perform a BLER < 0.1; however for wireless communications which is a power-limited system, high SNR cannot be performed by increasing indefinitely the eNodeB B power. Instead of selecting high data transmission modes with extremely bad quality and with less throughput, the base station can wisely and optimally rank 1 transmission modes i.e. CLSM rank 1 when the CSI is available or OLSM rank 1 when the CSI is not known.

The bad channel case corresponding to a degenerated MIMO channel is a trivial case i.e. if $\psi_{n,n_r} = 1$, SISO mode should be activated since MIMO channel behaves like SISO channel. Hence coding MIMO over SISO becomes useless and resource wasting.

8. Conclusion

For wireless radio propagation environments governed by scatterers, we present a channel modelling in this paper through the study of beamwidth generated scatterers. The framework based on beamwidth clustering, consists of associating an arbitrary beamwidth to a small cell. In principle, the physical parameter of a geometrical small ring of scatterers surrounding the User Equipment (UE) can be known at the base, however in fast fading scenario, the motion of the mobile inducing a relative virtual displacement of scatters and then a dynamic re-organization around the ring, introduces straightforward a stochastic features. For an arbitrary small cell, we extract MIMO channel correlation properties taking into account the stochastic features in terms of probability density function (PDF) of beamwidth. Both normal distribution and uniform distribution are considered to derive MIMO channel. As result, asymptotical characteristic in comparison with the reference model (one ring scattering channel model) are derived. Both BLER and throughput performances of MIMO spatial multiplexing and transmit diversity transmission modes are analysed over the channel model, revealing the optimal MIMO adaptive criterion.

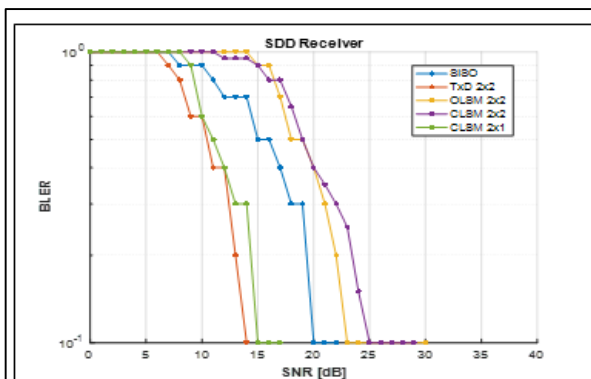


Fig.9 BLER in a Small Cell: $\alpha = 0.18; \psi = 0.0974$

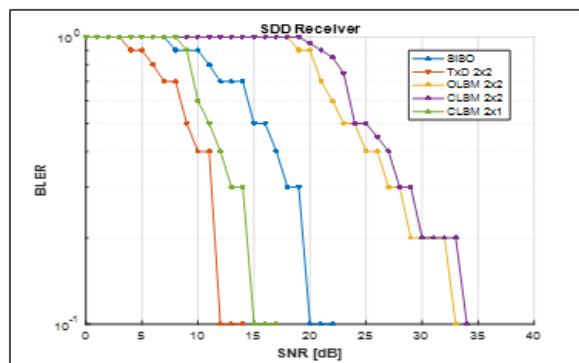


Fig.10. BLER in a Small Cell: $\alpha = 0.1; \psi = 0.4598$

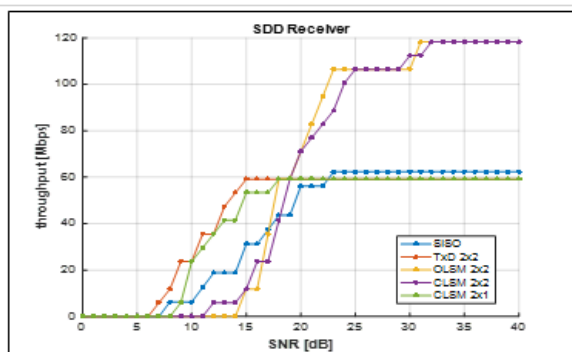


Fig.11. BLER in a Small Cell: $\alpha = 0.18; \psi = 0.0974$

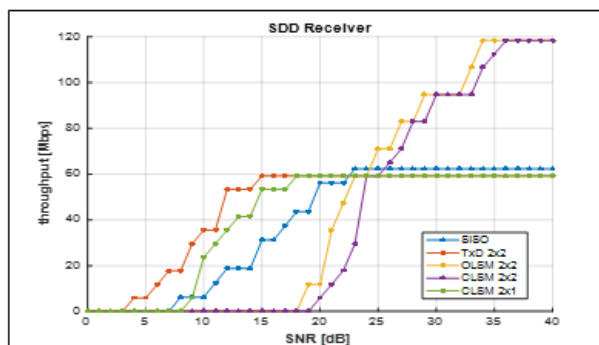


Fig.12. BLER in a Small Cell: $\alpha = 0.1; \psi = 0.4598$

Group of Figures.1: SDD receiver

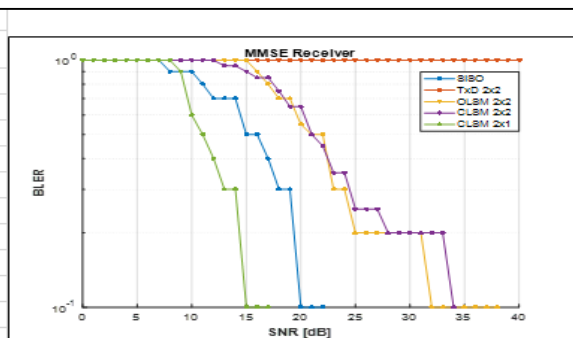


Fig.13 BLER in a Small Cell: $\alpha = 0.18; \psi = 0.0974$

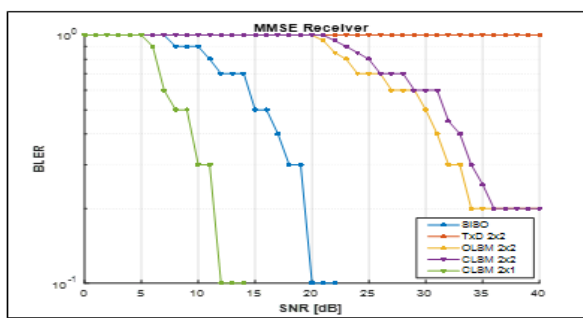


Fig.14 BLER in a Small Cell: $\alpha = 0.1; \psi = 0.4598$

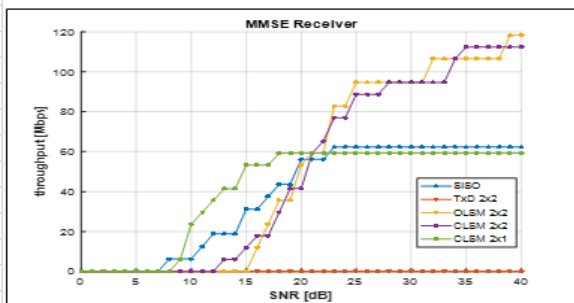


Fig.15 BLER in a Small Cell: $\alpha = 0.18; \psi = 0.0974$

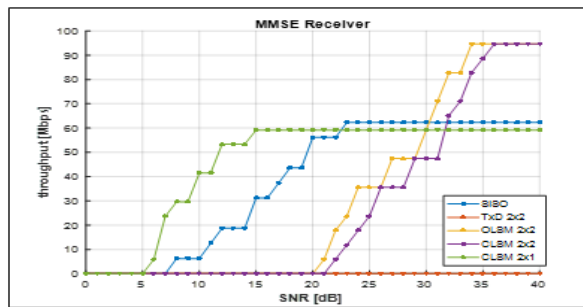
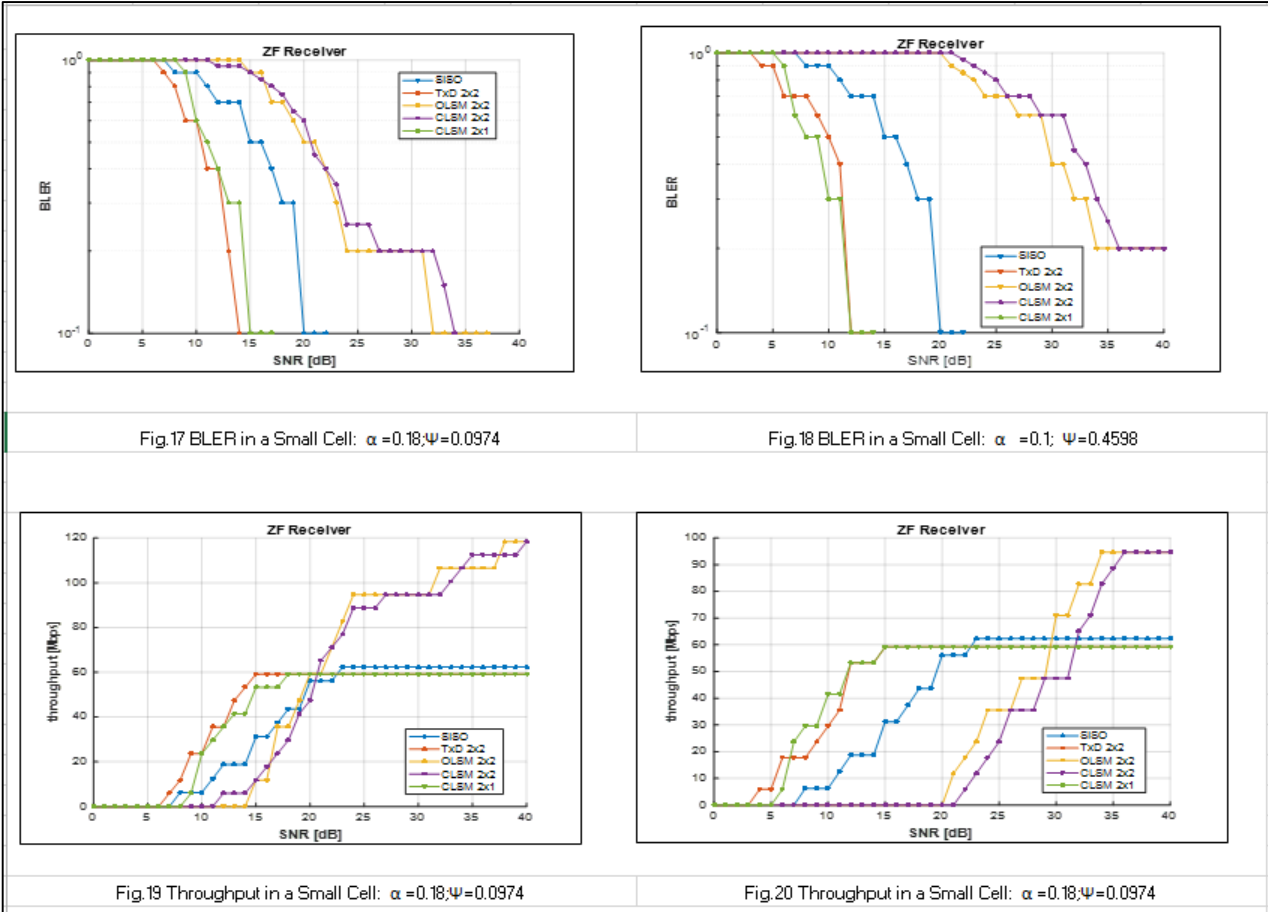


Fig.16 BLER in a Small Cell: $\alpha = 0.1; \psi = 0.4598$

Group of figures.2: MMSE Receiver



Group of figures.3 ZF Receiver

Appendix I General Mathematical Formulation of the One Ring Scattering Channel

In this appendix, we extend the formulation of the one ring scattering MIMO channel often limited to a 2x2MIMO configuration into an arbitrary n_t transmit and n_r received antenna. Assuming a plane wave with frequency f_c , the complex path gain between the l^{th} antenna at the mobile and the k^{th} antenna at the base station is denoted by $h_{k,l}(t)$ is [36][37][25]:

$$h_{k,l}(t) = \frac{1}{\sqrt{N}} \sum_{i=1}^N a_{il} b_{ik} \exp(j\phi_i) \exp[-j2\pi(f_d \cos(\theta_i - \beta) t)] \quad N \rightarrow \infty \quad (22)$$

With

$$a_{il} = e^{j\pi(3-2l)\frac{d}{\lambda} [\cos(\gamma_b) + \alpha \sin(\gamma_b) \sin(\theta_i)]} \quad (23)$$

$$b_{ik} = e^{j\pi(3-2k)\frac{D}{\lambda} [\cos(\theta_i - \gamma_m)]} \quad (24)$$

Where γ_m and γ_b denotes respectively the angle joining the mobile array and the x-axis at one side and the angle joining the base array and the x-axis at the other side.

The correlation $r_{kl,qs}(\Delta t)$ between two arbitrary MIMO sub channels $h_{k,l}(t)$ and $h_{q,s}(t)$ with a delay difference Δt can be written:

$$r_{kl,qs}(\Delta t) = \mathcal{E} \{ h_{k,l}(t) \cdot h_{q,s}^*(t + \Delta t) \} \quad (25)$$

where \mathcal{E} denotes the expectation.

Taking $p(\theta)$ as the probability density function in the angular domain of AOA, from (1), (3) we can rewrite following the transformation in [38][39]:

$$r_{kl,qs}(\Delta t, a, f_d) = \int_{-\pi}^{\pi} a_{il} a_{is}^* b_{ik} b_{iq}^* \exp[-j2\pi(f_d \cos(\theta_i - \beta) \Delta t)] \mathbf{X} p(\theta_i) d\theta_i \quad (26)$$

Where a_{is} and b_{iq} can be found simply by replacing in (23) and (24) l by s and k by q . Hence we can rewrite (26) as:

$$r_{kl,qs}(\Delta t, \alpha, f_d) = e^{j2\pi(s-l)\frac{d}{\lambda} \int_{-\pi}^{\pi} \exp\left[j2\pi\frac{d}{\lambda}(s-l)\alpha \sin \gamma_b \sin \theta_i\right] \times \exp\left[j2\pi\frac{D}{\lambda}(q-k)\cos(\theta_i - \gamma_m)\right] \times \exp[-j2\pi f_d \cos(\theta_i - \beta) \Delta t] p(\theta_i) d\theta_i}$$

The AOA $p(\theta)$ is often assumed following the Von Mises distribution [39]. For the computation in

(26), we assume the simple case of the distribution i.e. a uniform probability ($p(\theta) = 1/\pi$). Therefore, we derive:

$$r_{kl,qs}(\Delta t, \alpha, f_d) = e^{j2\pi(s-l)\frac{d}{\lambda} J_0} \left(2\pi \left(\left(\frac{D}{\lambda}(q-k)\sin \gamma_m + \frac{d}{\lambda} f_d \alpha (s-l) \sin \gamma_b - f_d \Delta t \sin \beta \right)^2 + \left(\frac{D}{\lambda}(q-k)\cos \gamma_m - f_d \Delta t \cos \beta \right)^2 \right)^{1/2} \right) \quad (27)$$

Where J_0 is the Bessel function of the first kind. q, k and s, l are integer numbers and can take values respectively from $[1, n_t]$ and $[1, n_r]$. All combinations are feasible and $r_{kl,qs}(\Delta t)$ can denote a transmit correlation, a receive correlation or a cross correlation, by setting up respectively $l \neq s, k=q; l=s, k \neq q$, and $l \neq s, k \neq q$. The combination of s, l and q, k should be done such that $s \geq l, q \geq k$.

Considering a parallel ($\gamma_m = \gamma_b = \pi/2$) Uniform Linear Array (ULA), we found in downlink transmission, the transmit correlation:

$$r_{kl,ks}(\Delta t, \alpha, f_d) = e^{j2\pi\frac{d}{\lambda} J_0} \left(2\pi \left(\frac{d}{\lambda} \alpha (s-l) + f_d \Delta t \right) \right) \quad (28)$$

The receive correlation:

$$r_{kl,ql}(\Delta t, \alpha, f_d) = J_0 \left(2\pi \left(\frac{D}{\lambda} (q-k) + f_d \Delta t \right) \right) \quad (29)$$

And the cross-correlation as:

$$r_{kl,qs}(\Delta t, \alpha, f_d) = e^{j2\pi\frac{d}{\lambda} J_0} \left(2\pi \left(\frac{D}{\lambda} (q-k) + \frac{d}{\lambda} \alpha (s-l) + f_d \Delta t \right) \right) \quad (30)$$

$k \neq q; l \neq s$

Appendix II

Elaboration of the Dynamic One-Ring Scattering Channel (DORSC) formula

In uniform PDF

In the reference model, an arbitrary one ring scattering channel in (24) $r_{kl,qs}(\alpha_n)$ is given:

$$r_{kl,qs}(\alpha_n) = e^{2\pi(s-l)\frac{d}{\lambda}} J_0 \left(2\pi \left(\frac{D}{\lambda} (q-k) + \frac{d}{\lambda} \alpha_n (s-l) + f_d \Delta t \right) \right)$$

Following [40], we can develop (27) in terms of Summation as:

$$r_{kl,qs}(\alpha_n) = e^{2\pi(s-l)\frac{d}{\lambda}} \left[J_0 \left(2\pi \left(\frac{D}{\lambda} (q-k) + f_d \Delta t \right) \right) J_0 \left(2\pi \frac{d}{\lambda} \alpha_n (s-l) \right) + 2 \sum_{N=1}^{+\infty} (-1)^N J_N \left(2\pi \left(\frac{D}{\lambda} (q-k) + f_d \Delta t \right) \right) \mathbf{X} J_N \left(2\pi \frac{d}{\lambda} \alpha_n (s-l) \right) \right] \quad (31)$$

Taking $\alpha_1=0$ and assuming the uniform PDF upon $\alpha_n = [\alpha_1, \alpha_3, \dots, \alpha_{\max}]$, and applying (31) in (13), the correlation $\overline{r_{kl,qs}}$ of dynamic one ring scattering channel model is as (13):

$$\overline{r_{kl,qs}} = \frac{1}{\alpha_1 - \alpha_{\max}} \int_{\alpha_1}^{\alpha_{\max}} r_{kl,qs}(\alpha_n) d\alpha_n$$

conducting to the $\overline{r_{kl,qs}}$ as:

$$\overline{r_{kl,qs}} = e^{j2\pi(s-l)\frac{d}{\lambda}} \frac{\lambda}{2\pi d(s-l)\alpha_{\max}} \left[J_0 \left(2\pi \left(\frac{D(q-k)}{\lambda} \pm f_d \Delta t \right) \right) \sum_{k=0}^{\infty} J_{2k+1} \left(\frac{2\pi}{\lambda} d(s-l)\alpha_{\max} \right) + 2 \left(\frac{s-l}{i} \right) \sum_{N=1}^{\infty} J_N \left(2\pi \left(\frac{D(q-k)}{\lambda} \pm f_d \Delta t \right) \right) \left(\sum_{k=0}^{\infty} J_{2k+N+1} \left(\frac{2\pi}{\lambda} d(s-l)\alpha_{\max} \right) \right) \right] \quad (32)$$

$$q = [1, n_t]; k = [1, n_t];$$

$$l = [1, n_r]; s = [1, n_r];$$

$$i = \left\{ \begin{array}{l} s-l \\ \text{with } s-l \neq 0 \end{array} \right\}$$

where the variable i is only used for a generalization purpose of the formula (32). The value of the multiplication between high orders Bessel function of the first kind decreases rapidly, therefore, we will only Take into account the first part of the equation (32), conducting to the following simplification:

$$\overline{r_{kl,qs}} = e^{j2\pi(s-l)\frac{d}{\lambda}} \frac{\lambda}{2\pi d(s-l)\alpha_{\max}} J_0 \left(2\pi \left(\frac{D(q-k)}{\lambda} \pm f_d \Delta t \right) \right) \sum_{k=0}^{\infty} J_{2k+1} \left(\frac{2\pi}{\lambda} d(s-l)\alpha_{\max} \right) \quad (14)$$

In Gaussian PDF Based DORSC

The correlation function $\overline{r_{kl,qs}}$ is computed assuming a Gaussian PDF of beamwidth:

$$d_n = \frac{2.c}{\sqrt{\pi}} e^{-c^2(\alpha_n - \alpha_0)^2}$$

Following the same rule of development of the computation methodology used above (for uniform PDF), we found the cross correlation $\overline{r_{kl,qs}}$ as:

$$\begin{aligned} \overline{r_{kl,qs}} &= \frac{1}{\sqrt{\pi}} e^{j2\pi(s-l)/\lambda} \cdot J_0 \left(2\pi \left(\frac{D(q-k)}{\lambda} \pm f_d \Delta t \right) \right) \cdot J_0 \left(\frac{2\pi}{\lambda} d(s-l)\alpha_0 \right) \sum_{m=0}^{\infty} \frac{(-1)^m \Gamma(m + \frac{1}{2})}{(2.c)^{2m} (m!)^2} + \sum_{p=1}^{\infty} J_p \left(2\pi \left(\frac{D(q-k)}{\lambda} \pm f_d \Delta t \right) \right) \\ &\times J_p \left(\frac{2\pi}{\lambda} d(s-l)\alpha_0 \right) \sum_{m=0}^{\infty} \frac{(-1)^m \Gamma(m + \frac{p}{2} + \frac{1}{2})}{(2.c)^{2m+p} m!(m+p)!} \end{aligned} \quad (33)$$

By neglecting the multiplication of high order of Bessel function, equation (30) respectively simplified like:

$$\overline{r_{kl,qs}} = e^{j2\pi(s-l)} \cdot J_0 \left(2\pi \left(\frac{D(q-k)}{\lambda} \pm f_d \Delta t \right) \right) \cdot \frac{1}{\sqrt{\pi}} J_0 \left(\frac{2\pi}{\lambda} d(s-l)\alpha_0 \right) \sum_{m=0}^{\infty} \frac{(-1)^m \Gamma(m + \frac{1}{2})}{(2.c)^{2m} (m!)^2} \quad (17)$$

References:

- [1] Y. Cemal and Y. Steinberg, "Coding Problems for Channels With Partial State Information at the Transmitter." IEEE TRANSACTIONS ON INFORMATION THEORY, VOL. 53, NO. 12, DECEMBER 2007
- [2] L.C.Wood and W.S. Hodgkiss, "Performance of MIMO Channel Models with Channel State Information at the Transmitter". IEEE "GLOBECOM" 2008 proceeding.
- [3] A. B. Gershman and N. D. Sidiropoulos, Space-Time Processing for MIMO Communications, England Wiley, pp.346-360, 2005, pp:323-324
- [4] W. Weichselberger, M. Herdin and H. Özcelik, "A Stochastic MIMO Channel Model With Joint Correlation of Both Link Ends," IEEE TRANSACTIONS ON WIRELESS COMMUNICATIONS, vol 5, No1, January 2006, pp.90-100.
- [5] Ericsson, "R4-060101: LTE Channel Models for Concept Evaluation in RAN1," TSG-RAN Working Group 4 (Radio) meeting 38 Denver, CO, February 13–17, 2006.
- [6] Commission of the European Communities, "IST-WINNER Project," <http://www.istwinner.org>.
- [7] Commission of the European Communities, IST-WINNER II Project Deliverable D1.1.2, V1.2 "WINNER II Channel Models," <http://www.ist-winner.org>
- [8] Technical Specification Group Radio Access Network; Physical Channels and Modulation, Release 9; 3GPP TS 36.211 V 9.1.0, March 2010 A.
- [9] Ericsson, Nokia, Motorola, and Rohde and Schwarz, "R4-070572: Proposal for LTE Channel Models," www.3gpp.org, 3GPP TSG RAN WG4, meeting 43, Kobe, Japan, May 2007.
- [10] Ericsson, "R4-070994—LTE Channel Models: High-speed Scenario," TSG-RAN Working Group 4 (Radio) meeting #43 bis Orlando, FL, June 25–29 2007.

- [11] D. Umansky and M. Patzold, 'Design of Measurement-Based Stochastic Wideband MIMO Channel Simulators', IEEE "GLOBECOM" 2009 proceedings
- [12] K. Yu, M. Bengtsson, B. Ottersten, D. McNamara, P. Karlsson and M. Beach, "Modeling of wide-band MIMO radio channels based on NLoS indoor measurements," IEEE Trans. Veh. Technol., vol. 53, no. 3.
- [13] I. Kolani, and J.Zhang, "MIMO Multi Ring Scattering Channel Model for Wireless Communications Macrocells", in Proc. IEEE 'ICIST', Wuhan, Hubei, China; March 23-25, 2012, pp 794-797
- [14] H. Ozelik, M. Herdin, W. Weichselberger, J. Wallace, and E. Bonek, "Deficiencies of 'Kronecker' MIMO radio channel model," Electron. Lett., vol. 39, no. 16, pp. 1209–1210, Aug. 2003.
- [15] Y. Ma and M. Patzold, "Performance comparison of space-time coded MIMO–OFDM systems using different wideband MIMO channel models," in Proc. 4th IEEE International Symposium on Wireless Communication Systems, ISWCS 2007. Trondheim, Norway, Oct. 2007, pp. 762–766.
- [16] S. Guerin, "Indoor wideband and narrowband propagation measurements around 60.5 GHz in an empty and furnished room," in Proc. 46th Vehicular Technology Conference, VTC 1996-Spring, vol. 1. Atlanta, GA, Apr. 1996, pp. 160–164.
- [17] I. Kolani, J.Zhang and G. zehua, "MIMO Channel Modeling: Covariance estimation based on multi ring scattering environments", in Proc. IEEE 'WICOM', Shanghai 2012
- [18] M. Patzold and B. O. Hogstad, "A wideband MIMO channel model derived from the geometric elliptical scattering model," in Proc. 3rd International Symposium on Wireless Communication System, ISWCS 2006. Valencia, Spain, Sept. 2006, pp. 138–144.
- [19] D. S. Baum, J. Salo, G. Del Galdo, M. Milojevic, P. Kyosti, and J. Hansen, "An Interim Channel Model for Beyond-3G Systems," in Proc. IEEE Vehicular Technology Conference, Stockholm, May 2005
- [20] P. Almers, E. Bonek, A. Burr, N. Czink, M. Debbah, V. Degli-Esposti, H. Hofstetter, P. Kyosti, D. Laurenson, G. Matz, A. F. Molisch, C. Oestges, and H. Ozelik, "Survey of Channel and Radio Propagation Models for Wireless MIMO Systems," EURASIP Journal on Wireless Communications and Networking (special issue on space-time channel modelling for wireless communications), 2007.
- [21] L. Song and J. Shen, Evolved cellular network planning and optimization for UMTS and LTE, pp:66-81, 2011 by Taylor and Francis Group, LLC CRC Press is an imprint of Taylor & Francis Group, an Informa business
- [22] C. Chen, and M. A. Jensen, "A Stochastic Model of the Time-Variant MIMO Channel Based on Experimental Observations", IEEE TRANSACTIONS ON VEHICULAR TECHNOLOGY, VOL. 58, NO. 6, pp2618-2625, JULY 2009.
- [23] X. Cheng and D. I. Laurenson, "Multiple-Ring Based Modeling and Simulation of Wideband Space-Time-Frequency MIMO Channels", 978-1-4244-3435-0/09/\$25.00 ©2009 IEEE.
- [24] X. Cheng, C.-X. Wang, and D. I. Laurenson, "A generic space-time frequency correlation model and its corresponding simulation model for MIMO wireless channels," 2nd EuCAP 2007, Edinburgh, Scotland, U.K., Nov. 2007, pp. 1–6.
- [25] M. Patzold and B. O. Hogstad, "A wideband space-time MIMO channel simulator based on the geometrical one-ring model," in Proc. 64th Vehicular Technology Conference, VTC 2006-Fall. Montreal, Canada, Sept. 2006.
- [26] W. C. Jakes Jr, "Multipath interference," in Microwave Mobile Communications, W. C. Jakes Jr., Ed. New York: Wiley, 1974, pp. 11–78.
- [27] W. C. Y. Lee, "Effects on correlation between two mobile radio base-station antennas," IEEE Trans. Commun., vol. 21, pp. 1214–1224, 1973.
- [28] A. Abdi and M. Kaveh, "Space-time correlation modeling of multielement antennas systems in mobile fading channels," in Proc. ICASSP2001, Salt Lake City, Utah, May 2001.
- [29] K. I. Pedersen, P. E. Mogensen, and B. H. Fleury, "A stochastic model of the temporal and azimuthal dispersion seen at the base station in outdoor propagation environments," IEEE Trans. Vehic. Technol., vol. 49, pp. 437–447, 2000.
- [30] U. Martin, "Spatio-temporal radio channel characteristics in urban macrocells," IEE Proc. Radar, Sonar, Navig., vol. 145, pp. 42–49, 1998.
- [31] P. Pajusco, "Experimental characterization of D.O.A at the base station in rural and urban area," in Proc. IEEE Veh. Technol. Conf., Ottawa, ON, Canada, 1998, pp. 993–997.
- [32] T. S. Chu and L. J. Greenstein, "A semi-empirical representation of antenna diversity

- gain at cellular and PCS base stations,” IEEE Trans. Commun., vol. 45, pp. 644–646, 1997.
- [33] K. Yu, Multiple-Input Multiple-Output radio propagation channels: Kronecker’s model. Characteristics and models. Ph.D. thesis, Royal Institute of Technology, 2005, Stockholm
- [34] M. T. Ivrlac and J. A. Nossek, ‘Diversity and Correlation in Rayleigh Fading MIMO Channels’, in Proc .3rd IEEE Int .Symp.on Signal Processing and Information Technology,(ISSPIT),pages:158-161,Darmstadt ,Germany ,December 2003.
- [35] M. T. Ivrlac, “Measuring Diversity and Correlation in Rayleigh Fading MIMO Communication Systems”, Technical Report No: TUM-LNS-TR-03-04, Munich University of Technology, April 2003
- [36] W.HAKIMI, M. AMMAR, A. BOUALLEGUE and S. SAOUDIA, “Generalized Wideband Space-Time MIMO Channel Simulator Based on the Geometrical Multi-Radii One-Ring Model”,978-1-4244-1645-5/08/\$25.00 ©2008 IEEE, pp: 1266-1270.
- [37] Y. Ma and M. Patzold, “A Wideband One-Ring MIMO Channel Model Under Non-Isotropic Scattering Conditions”, 978-1-4244-1645-5/08/\$25.00 ©2008 IEEE, pp: 424-429.
- [38] I. Kolani, J.Zhang and G. zehua, “Amount of Correlation Function-based Diversity Motivation Design in MIMO Systems”, International Journal of Information and Computer Science,2012 IJICS Volume 1, Issue 6, September 2012 PP. 159-162
- [39] Z. Latinovic, A. Abdi, and Y. Bar-Ness, ‘A Wideband Space-Time Model for MIMO Mobile Fading Channels’0-7803-7700-1/03/\$17.00 (C) 2003 IEEE.
- [40] M. R. SPIEGEL, Schaum’s Mathematical Handbook of Formulas and Table Rensselaer Polytechnic Institute September, 1968.
- [41] Fa-Long Luo and Jianzhong Zhang, signal processing for 5G: Algorithms and Implementation, 2016 John Wiley & Sons, Ltd
- [42] Vienna LTE Simulators Link Level Simulator Documentation, v1.7r1089, Institute of Telecommunications Vienna University of Technology, Austria Gusshausstrasse 25/389, A-1040 Vienna, Austria Email: {fjcolom, msimko, sschwarzg@nt.tuwien.ac.at} Web:<http://www.nt.tuwien.ac.at/ltesimulator>